Phenolsulfonphthalein, but Not Phenolphthalein, Inhibits Amyloid Fibril Formation: Implications for the Modulation of Amyloid Self-Assembly†

Michal Levy,‡,§ Yair Porat,‡,§,|| Eran Bacharach,⊥ Deborah E. Shalev,# and Ehud Gazit*,‡

Department of Molecular Microbiology and Biotechnology and Department of Cell Research and Immunology, George S. Wise Faculty of Life Sciences, Tel Aviv University, Tel Aviv 69978, Israel, and The Wolfson Centre for Applied Structural Biology, Safra Campus, The Hebrew University of Jerusalem, Givat Ram, Jerusalem 91904, Israel

Received January 8, 2008; Revised Manuscript Received April 6, 2008

ABSTRACT: The study of the mechanism of amyloid fibril formation and its inhibition is of key medical importance due to the lack of amyloid assembly inhibitors that are approved for clinical use. We have previously demonstrated the potent inhibitory potential of phenolsulfonphthalein, a nontoxic compound that was approved for diagnostic use in human subjects, on aggregation of islet amyloid polypeptide (IAPP) that is associated with type 2 diabetes. Here, we extend our studies on the mechanism of action of phenolsulfonphthalein by comparing its antiamyloidogenic effect to a very similar compound that is also approved for human use, phenolphthalein. While these compounds have very similar primary chemical structures, they significantly differ in their three-dimensional conformation. Our results clearly demonstrated that these two compounds had completely different inhibitory potencies: While phenolsulfonphthalein was a very potent inhibitor of amyloid fibril formation by IAPP, phenolphthalein did not show significant antiamyloidogenic activity. This behavior was observed with a short amyloid fragment of IAPP and also with the full-length polypeptide. The NMR spectrum of $IAPP_{20-29}$ in the presence of phenolsulfonphthalein showed chemical shift deviations that were different from the unbound or phenolphthalein-bound peptide. Differential activity was also observed in the inhibition of insulin amyloid formation by these two compounds, and density-gradient experiments clearly demonstrated the different inhibitory effect of the two compounds on the formation of prefibrillar assemblies. Taken together, our studies suggest that the three-dimensional arrangement of the polyphenol phenolsulfonphthalein has a central role in its amyloid formation inhibition activity.

Over twenty amyloid-associated diseases have been characterized to date, among them type 2 diabetes, systemic amyloidosis, and various neurodegenerative disorders such as Alzheimer's disease and Parkinson's disease (*1, 2*). A common feature of these diseases is self-assembly of usually monomeric proteins to fibrillar structures that aggregate in large microscopic deposits in the affected tissues and organs (*3, 4*). These deposits are characterized by accumulations of fibrillar structures with distinct elongated morphology of 5−15 nm in diameter, cross β-sheet conformation, and typical X-ray fiber diffraction (*5*).

Human islet amyloid polypeptide (hIAPP[1]) is cosecreted with insulin. In type 2 diabetes hIAPP forms extracellular pancreatic deposits once insulin resistance results in the overexpression of insulin, leading to loss of β-cell function and finally cell death. Postmortem examination shows that more than 95% of type 2 diabetes pancreatic tissue is characterized by large IAPP deposits (*6, 7*). Although it is unclear whether fibril and deposit formation are the cause or result of the disease, many recent findings have suggested that prefibrillar assemblies (also termed oligomers) are more cytotoxic than mature fibrils (*8*). Therefore, finding an inhibitor that will specifically inhibit the early stages of amyloid fibril formation is of great therapeutic value (*9*).

Various small molecules have been reported to inhibit amyloid fibril formation including a prominent group of polyphenol compounds (*10*). Polyphenols have been shown to inhibit different amyloidogenic proteins *in vitro*, in cell culture, and recently *in vivo* (*11, 12*). Interestingly, several polyphenols were shown to inhibit more than one amyloidogenic protein; e.g. tannic acid was shown to inhibit β-amyloid and prion PrP^{sc}; dobutamine was shown to inhibit α-synuclein and huntingtin, and epicatechin gallate was

† The work was supported by the BIO-DISK and DIP (Deutsch-Israelische Projektkooperation) grants to E.G.

* To whom correspondence should be addressed. Mailing address: Department of Molecular Microbiology and Biotechnology, George S. Wise Faculty of Life Sciences, Tel Aviv University, Tel Aviv 69978, Israel. E-mail: ehudg@post.tau.ac.il. Tel: +972-3-640-9030. Fax: +972-3-640-5448.

‡ Department of Molecular Microbiology, George S. Wise Faculty of Life Sciences, Tel Aviv University.

§ These authors equally contributed to this work.

|| Current address: Division of Neurobiology, Johns Hopkins University School of Medicine, 600 North Wolfe Street, Baltimore, MD 21287.

⊥ Department of Cell Research and Immunology, George S. Wise Faculty of Life Sciences, Tel Aviv University.

The Hebrew University of Jerusalem.

[1] Abbreviations: IAPP, islet amyloid polypeptide; TEM, transmission electron microscopy; DMSO, dimethyl sulfoxide; HFIP, 3,3,3,3′,3′,3′-hexafluoro-2-propanol.

10.1021/bi800043d CCC: $40.75
Published on Web 05/06/2008

shown to inhibit β-amyloid and Tau (for further details see review by Porat et al. (*13*)).

A potent therapeutic inhibitor must have high efficacy, be safe for continuous administration, and interact specifically with amyloidogenic structures (*9*). We have previously reported that phenolsulfonphthalein, a small synthetic polyphenol which is commonly used as a pH indicator in cell culture assays and medical procedures, dose-dependently inhibited fibril formation by IAPP *in vitro* with an IC_{50} value of 1 μM (*14*). Furthermore, phenolsulfonphthalein inhibited IAPP cytotoxicity toward pancreatic rodent β-cells, and increased cell viability by 30% when IAPP was added to the cell growth medium (*14*).

Phenolsulfonphthalein has been used clinically since the early 1960s as a diagnostic marker for testing renal function (PSP test) by estimating the rate of excretion in urine after intravenous injection (*15*). Phenolsulfonphthalein is also used to improve the accuracy of gastric secretion studies (*16*) and for patency evaluation of the fallopian tubes (*17*). The toxicity data is well characterized and LD_{50} values are established both intravenously (rat LD_{50}, 752 mg/kg; mouse LD_{50}, 1368 mg/kg (*34*)) and subcutaneously (rat LD_{50}, >600 mg/kg (*35*), 185, 1971).

Here we provide further experimental evidence that phenolsulfonphthalein is an efficient and specific inhibitor of amyloid formation *in vitro*, using spectroscopic aggregation assay, electron microscopy and density gradient fractionation assay. We demonstrate that a very similar molecule, phenolphthalein (Figure 1), does not have similar inhibitory effect. We also show differences in the amyloid interaction with phenolsulfonphthalein and phenolphthalein by NMR spectroscopy: The spectrum of $hIAPP_{20-29}$ in the presence of phenolsulfonphthalein showed chemical shift deviations for Ile26 and Phe23 that were different from the unbound or phenolphthalein-bound peptide.

MATERIALS AND METHODS

Peptide Synthesis and Preparation of Stock Solutions. All peptide syntheses were performed using solid-phase methods by Peptron Inc. (Taejeon, Korea) for the $hIAPP_{22-29}$ and $hIAPP_{20-29}$ peptide and by Calbiochem for $hIAPP_{1-37}$ polypeptide. The correct identity of the peptides was confirmed by ion spray mass spectrometry, and the purity of the peptides was confirmed by reverse phase high-pressure liquid chromatography and NMR in the case of $hIAPP_{20-29}$. $hIAPP_{22-29}$ and $hIAPP_{20-29}$ stock solutions were prepared by dissolving the lyophilized form of the peptides in dimethyl sulfoxide (DMSO) at a concentration of 100 mM. The stock solution for $hIAPP_{1-37}$ was prepared by dissolving the lyophilized form of the peptide in 3,3,3,3′,3′,3′-hexafluoro-2-propanol (HFIP) at a concentration of 400 μM. To avoid any preaggregation, all stock solutions were sonicated for 2 min before each experiment. MALDI-TOF mass spectrometry analysis (using an Applied Biosystems Voyager DE-STR spectrometer) showed no fragmentation of the polypeptide after sonication.

Kinetic Aggregation Assay. The $hIAPP_{22-29}$ or $hIAPP_{20-29}$ peptide stock solutions were diluted into 10 mM Tris-HCl (pH 7.2) buffer to a final concentration of 1 mM peptide and 4% DMSO. Phenolsulfonphthalein and phenolphthalein were dissolved in ethanol and diluted in the same buffer to a final concentration of 10 mM. A similar concentration of ethanol was used in the control. Turbidity was measured at 560 nm at room temperature using disposable UVette cuvettes (Eppendorf, Germany) using a Scinco S-3100 spectrophotometer. At this wavelength the absorbance of the control samples, which contained the inhibitors in buffer alone, was steady throughout the experiments.

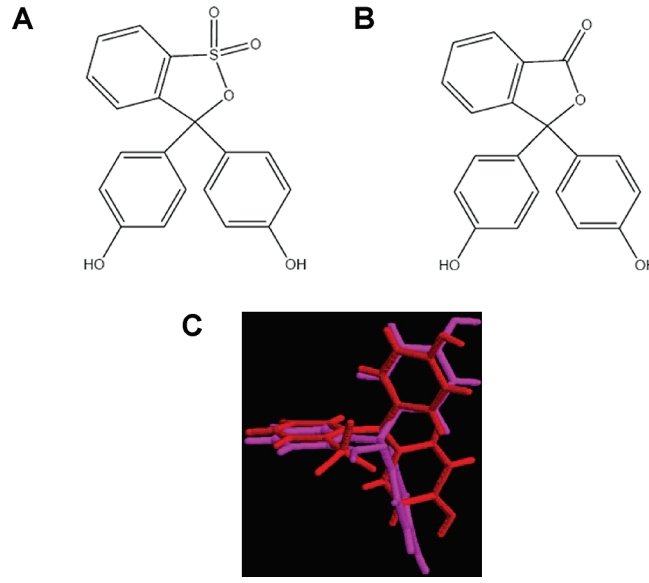

FIGURE 1: The chemical structures of (A) phenolsulfonphthalein and (B) phenolphthalein and (C) comparison of the three-dimensional conformations of phenolsulfonphthalein and phenolphthalein.

Thioflavin T Fluorescence Assay. A stock solution of synthetic $hIAPP_{1-37}$ was diluted to a final concentration of 4 μM in 10 mM sodium acetate buffer (pH 6.5) with or without inhibitor (40 μM), and a final HFIP concentration of 1% (v/v). Immediately after dilution, the sample was centrifuged at 4 °C for 20 min at 20000*g*, and the supernatant was used for fluorescence measurements. Thioflavin T was added to a final concentration of 3 μM. 100 μM of bovine insulin were dissolved in double distilled water (DDW) at pH 2 (titrated by sulfonic acid), and diluted 2× with phenolsulfonphthalein that was dissolved in the same solution in ascending concentrations of 0−100 μM, to a final concentration of 50 μM. The mixture was then heated for 48 h to 50 °C. Thioflavin T was added to a final concentration of 4 μM. All samples were diluted 10-fold and measured using a Jobin Yvon Horiba Fluoromax 3 fluorimeter (excitation at 450 nm, 2.5 nm slit; emission at 480 nm, 5 nm slit). No fluorescence quenching was caused due to the presence of the inhibitors. In addition, the fluorescence values of the solutions containing the inhibitors alone were steady throughout the experiments.

Transmission Electron Microscopy. Samples (10 μL) of $hIAPP_{22-29}$ and $hIAPP_{20-29}$ from the aggregation assay, or $hIAPP_{1-37}$ from the fluorescence assay, were placed on 400-mesh copper grids (SPI supplies, West Chester, PA) covered by carbon-stabilized Formvar film. After 1 min, excess fluid was removed and the grids were negatively stained with 2% uranyl acetate in water for another two minutes. Samples were viewed in a JEOL 1200EX electron microscope operating at 80 kV.

Density Gradient Fractionation Assay. Bovine insulin (Sigma) was dissolved in DDW at pH 2 (sulfonic acid), and

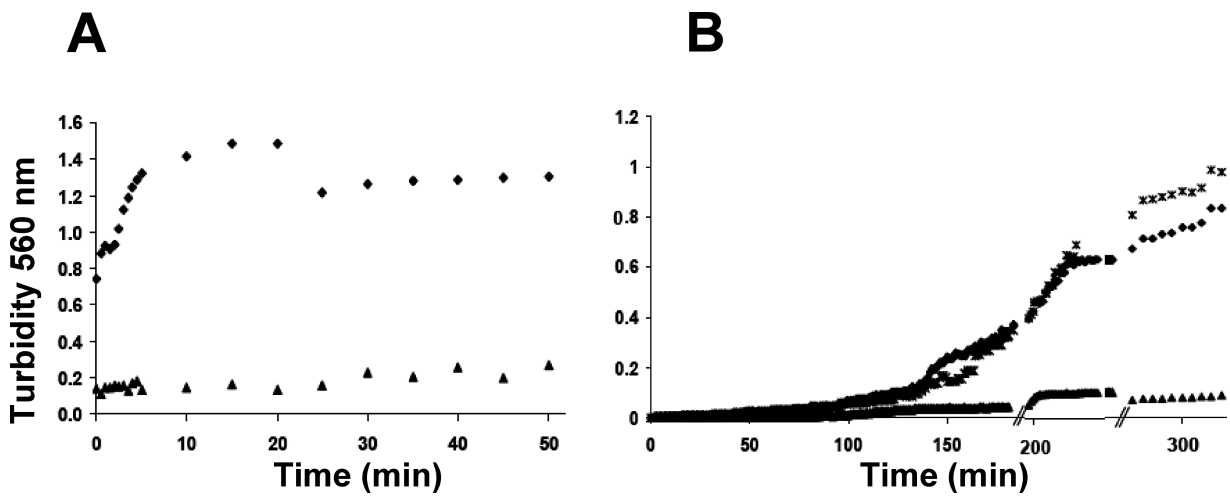

FIGURE 2: Inhibition of $hIAPP_{20-29}$ and $hIAPP_{22-29}$ peptides with phenolsulfonphthalein and phenolphthalein (inhibitor:peptide molar ratio of 10:1) using aggregation assay. (A) NFGAILSS peptide alone (◆), and in the presence of phenolsulfonphthalein (▲). (B) SNNFGAILSS alone (◆), in the presence of phenolsulfonphthalein (▲), and in the presence of phenolphthalein (∗). Turbidity at 560 nm was measured continuously for each sample, and background values of the buffer or inhibitor were subtracted from the relevant measurement. // represents vortexing of the samples.

diluted 2× with inhibitors or buffer to a final concentration of 50 μM. Phenolsulfonphthalein and phenolphthalein were dissolved in ethanol and diluted to a concentration of 100 μM with DDW pH 2, and finally diluted to 50 μM with an insulin solution. The mixture was then incubated for 48 h at 50 °C. A continuous density gradient of 3 mL volume was built using a 15 mL gradient maker (Hoefer, Inc.) with optiprep solution (Sigma) and DDW pH 2 (top-minimal density, bottom-maximal density), with slight changes to the method reported (*18*). After incubation, 0.6 mL of each sample was placed on top of the gradient and samples were centrifuged for 24 h at 150000*g* using a Beckman LE-70 Ultracentrifuge, SW60 rotor. Fractionation was done from the top (fraction 1) to bottom (fraction 9) by upward displacement, 0.36 mL per fraction. 0.2 mL of each fraction was blotted on nitrocellulose paper using a slot blot apparatus, stained with Ponceau red solution, and, after washing, incubated with anti-insulin antibody H-86 (Santa Cruz, USA) as the primary antibody and with antimouse HRP (Jackson) as a secondary antibody. Insulin fibril formation was measured using Thioflavin T fluorescence as described above.

NMR Measurements. All samples were stored in lyophilized form and were dissolved first in d_6-DMSO, and then triple-distilled water titrated with HCl to pH 4.0 was added to obtain a 1.1 mM concentration in 20% (v/v) d_6-DMSO in acidic water solution. When ligands were added, they were dissolved in d_6-DMSO, mixed with the d_6-DMSO solution of $hIAPP_{20-29}$, and then acidic water was added as described above to reach a 4:1 molar ratio of ligand to peptide. The apparent pH values for the samples were 3.8, 3.9 and 4.0 for $hIAPP_{20-29}$, $hIAPP_{20-29}$ with phenolphthalein and $hIAPP_{20-29}$ with phenolsulfonphthalein, respectively. Reference samples with phenolphthalein and phenolsulfonphthalein at the same concentrations both had pH values of 4.0. NMR experiments were performed on a Bruker Avance 600 MHz DMX spectrometer operating at the proton frequency of 600.13 MHz using a 5 mm selective probe equipped with a self-shielded xyz-gradient coil. Data was acquired at 25 °C. The residual water resonance was suppressed using a Watergate sequence for TOCSY (*19*) experiments which were recorded using the MLEV-17 pulse scheme for the spin lock and a mixing time of 150 ms. The water signal was used as a reference and was calibrated at 4.77 ppm. Zero filling in the t_1 dimension and data apodization with a shifted squared sine bell window function in both dimensions were applied prior to Fourier transformation. The baseline was further corrected in the F_2 dimension with a quadratic polynomial function. Spectra were processed and analyzed with the XWINNMR software package (Bruker Analytische Messtechnik GmbH).

The sequence gives unambiguous resonance assignments apart from the two serine residues. The 1D spectra were acquired under the same conditions of temperature, pH, concentration, and acquisition parameters and were compared using the XWINNMR program.

RESULTS

Inhibition Effect of Phenolsulfonphthalein on hIAPP Core Amyloidogenic Peptides. The core amyloidogenic fragments of hIAPP, $hIAPP_{20-29}$ and $hIAPP_{22-29}$ (NFGAILSS and SNNFGAILSS) aggregate quickly in aqueous solution, such that aggregation is a preliminary assay for amyloid formation (*20*). In order to have an evaluation of the inhibitory effect of phenolsulfonphthalein on hIAPP core peptide fibril formation, we compared the aggregation of 1 mM $hIAPP_{22-29}$ and $hIAPP_{20-29}$ with or without 10 mM phenolsulfonphthalein. To verify the specificity of phenolsulfonphthalein toward hIAPP core peptides, a very similar molecule—phenolphthalein, which differs only by the lack of the sulfone group—was used as a control (Figure 1).

The rate of aggregation of $hIAPP_{20-29}$ is slower than that of $hIAPP_{22-29}$, and an approximately 2 h lag time is evident in all samples. No inhibition effect was evident using $hIAPP_{20-29}$ with phenolphthalein, and its turbidity curve is similar to that of $hIAPP_{20-29}$ aggregation, which increased dramatically after 3 h (Figure 2B). Phenolsulfonphthalein inhibited all changes in aggregation although a slight elevation in aggregation levels is evident after 3 h (Figure 2B).

$hIAPP_{22-29}$ aggregated within seconds, and its turbidity reached a plateau after 10 min (Figure 2A). Aggregation of

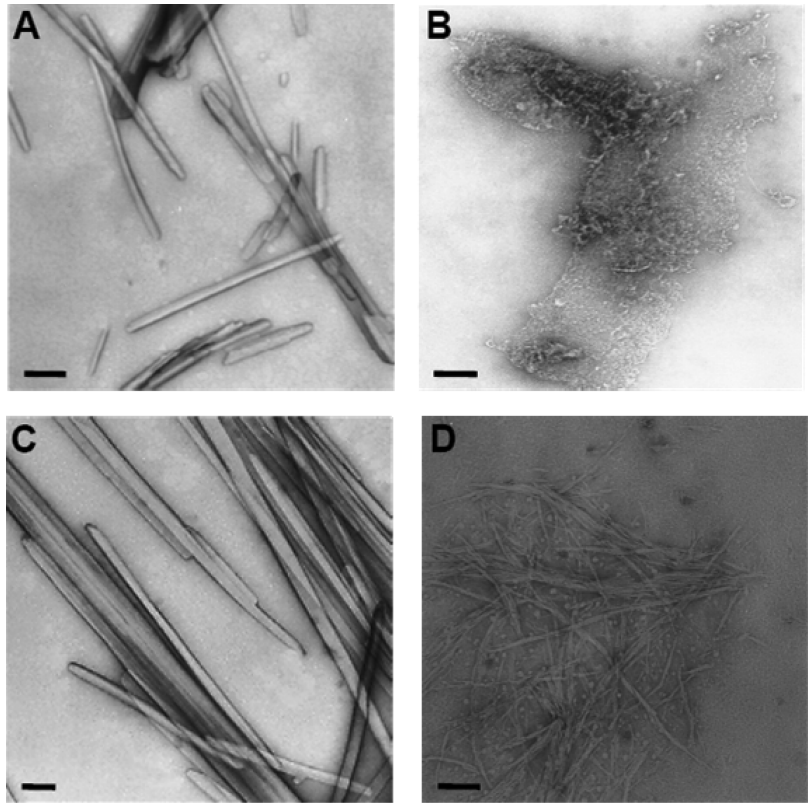

FIGURE 3: Morphology of $hIAPP_{22-29}$ fibrils with phenolsulfonphthalein (inhibitor:peptide molar ratio of 10:1): Distinct morphological differences are evident between the peptide alone and peptide that was aggregated in the presence of phenolsulfonphthalein. NFGAILSS peptide after (A) 3 and (C) 72 h. NFGAILSS peptide aggregated in the presence of phenolsulfonphthalein, after (B) 3 and (D) 72 h. Bar represents 100 nm.

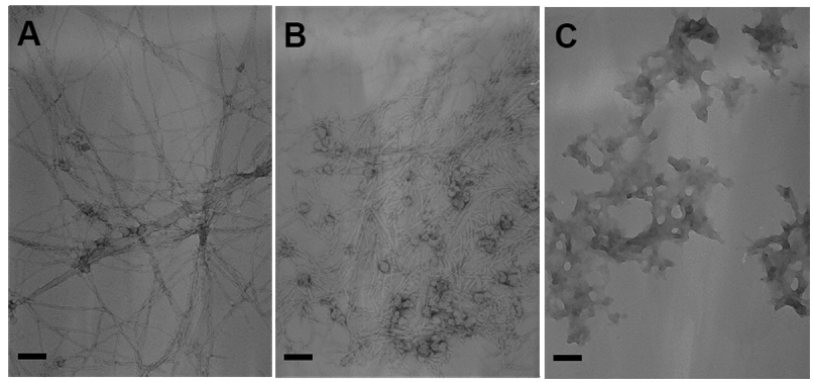

FIGURE 4: Ultrastructural morphology of $hIAPP_{20-29}$ fibrils with phenolsulfonphthalein and phenolphthalein. Distinct morphological differences are evident for fibril morphology between 1 mM SNNFGAILSS (A) without inhibitor and the same (B) with 10 mM phenolsulfonphthalein. In contrast, no inhibition effect is evident by addition of (C) 10 mM phenolphthalein. Bar represents 100 nm.

$hIAPP_{22-29}$ in the presence of phenolsulfonphthalein was practically stopped and much lower and constant levels of turbidity were present during the entire assay (Figure 2A).

Morphology of hIAPP Core Peptide Fibrils with and without Phenolsulfonphthalein Using TEM. To verify that aggregation results represent amyloid fibril formation, samples of $hIAPP_{20-29}$ and $hIAPP_{22-29}$ taken from the aggregation assay were viewed using electron microscopy. The $hIAPP_{22-29}$ samples were viewed 3 and 72 h after aggregation was initiated (Figure 3). Distinct and well-defined amyloid fibrils were present both in the 3 and 72 h samples of the $hIAPP_{22-29}$ peptide, with a minor increase in fiber density and width after 72 h. In contrast to the distinct morphology of the peptide alone, when phenolsulfonphthalein was used as inhibitor, no fibrils were seen after 3 h and some fibrils with different morphology were seen after 72 h.

$hIAPP_{20-29}$ aggregates were seen after 24 h with phenolsulfonphthalein and phenolphthalein as inhibitors (Figure 4). Characteristic amyloid fibrils that resemble $hIAPP_{1-37}$ fibrils were formed by 1 mM $hIAPP_{20-29}$ peptide alone (Figure 4A). Adding 10 mM of phenolphthalein did not interrupt fibril formation, and mature fibrils, which were assembled in bundles, were present on the transmission electron microscopy (TEM) grid (Figure 4B). This result confirmed the noninhibitory effect of phenolphthalein obtained by the aggregation assay. In contrast to the characteristic morphology of $hIAPP_{20-29}$ peptide without inhibitor compound, adding phenolsulfonphthalein inhibited fibril formation and

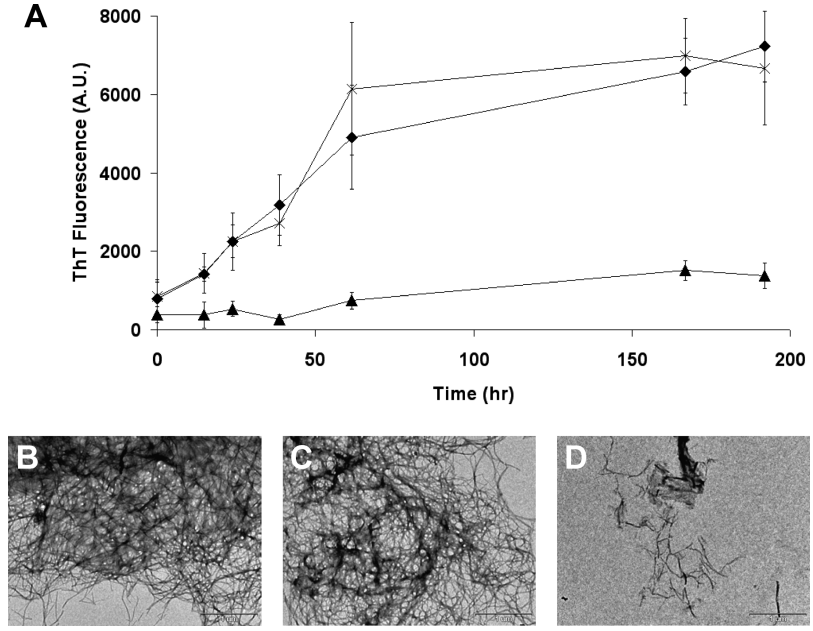

FIGURE 5: Inhibition of hIAPP with phenolsulfonphthalein or phenolphthalein using fluorescence assay and TEM. (A) Thioflavin T fluorescence assay of 4 μM hIAPP incubated alone (◆), with 40 μM phenolsulfonphthalein (▲) and 40 μM phenolphthalein (∗). Samples from the fluorescence assay were viewed using TEM. Dense characteristic fibrils were visible both for hIAPP (B) alone and (C) after addition of 40 μM phenolphthalein molecule. (D) In contrast, only rare and morphological altered fibrils were visible after inhibition with 40 μM phenolsulfonphthalein. Bar represents 1 μm.

none were seen after 24 h (Figure 4C). The aggregates formed by adding phenolsulfonphthalein to $hIAPP_{20-29}$ show some degree of order, but did not resemble the characteristic amyloid fibrils formed by the peptide alone or in the presence of phenolphthalein.

Inhibition of $hIAPP_{1-37}$ Fibril Formation with Phenolsulfonphthalein and Phenolphthalein. Previous results have shown that adding phenolsulfonphthalein to $hIAPP_{1-37}$ had a dose-dependent inhibitory effect on fibril formation *in vitro* (*14*). To evaluate the specificity of phenolsulfonphthalein toward $hIAPP_{1-37}$, phenolphthalein was used as a control. Thioflavin T fluorescence assay, which is a common assay for evaluating fibril formation, was performed with 4 μM $hIAPP_{1-37}$, and 40 μM of phenolsulfonphthalein or phenolphthalein. As shown in Figure 5A, phenolphthalein had no inhibitory effect on $hIAPP_{1-37}$ compared to that of phenolsulfonphthalein. This result is in agreement with previous results in Figures 2B and 4 for the SNNFGAILSS peptide ($hIAPP_{20-29}$). Furthermore, TEM micrographs of the same samples clearly show that amyloid fibrils were formed while using phenolphthalein as an inhibitor (Figure 5C) and only few and noncharacteristic fibrils were formed while using phenolsulfonphthalein (Figure 5D).

Phenolsulfonphthalein Inhibits Insulin Fibril Formation in a Dose-Dependent Manner. To verify whether the phenolsulfonphthalein inhibitory effect is specific to hIAPP or behaves as other polyphenols that inhibit multiple amyloidogenic proteins, we characterized the inhibitory effect of phenolsulfonphthalein on insulin under amyloid-forming conditions. Insulin forms characteristic amyloid fibrils at low pH and high temperatures and therefore serves as a good model for amyloid fibril formation. 50 μM of bovine insulin in DDW pH 2 (titrated by sulfonic acid) was incubated with ascending concentrations of phenolsulfonphthalein ranging from 0 μM to 100 μM. Insulin solutions were heated for 48 h to 50 °C, and insulin fibril formation was measured

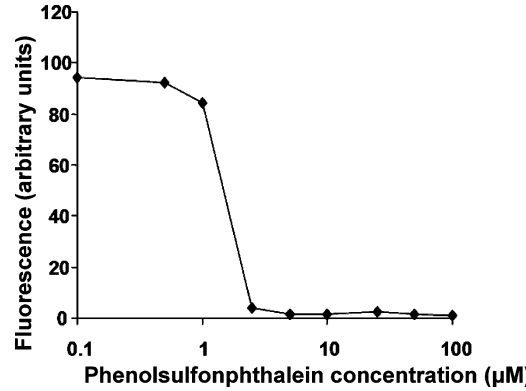

FIGURE 6: Concentration-dependent inhibition of insulin fibril formation using Thioflavin T assay. Thioflavin T fluorescence assay of insulin 50 μM was incubated for 48 h with ascending concentrations of phenolsulfonphthalein.

using Thioflavin T fluorescence. The dose-dependent inhibition curve (Figure 6) demonstrates that phenolsulfonphthalein inhibits insulin amyloid fibril formation in a dose-dependent manner with an IC_{50} value of 1.5 μM.

Density Gradient Fractionation of Fibrillar and Prefibrillar Intermediates of Amyloidogenic Insulin. Fractionation of the different intermediates of the amyloidogenic protein aggregation pathway is an efficient tool to study the exact influence of inhibitors on the different stages of fibril formation. We used density gradients and ultracentrifugation, based on the protocol by Ward et al. (*18*), to fractionate amyloidogenic insulin that was preincubated for 48 h under amyloid-inducing conditions with and without inhibitors. After ultracentrifugation and separating the fractions, each fraction was analyzed for its Thioflavin T fluorescence, and after blotting (using slot-blot), anti-insulin antibody was used to determine the presence of insulin, and Ponceau red was used to determine protein concentration (Figure 7). Insulin alone presented a very clear fractionation pattern where

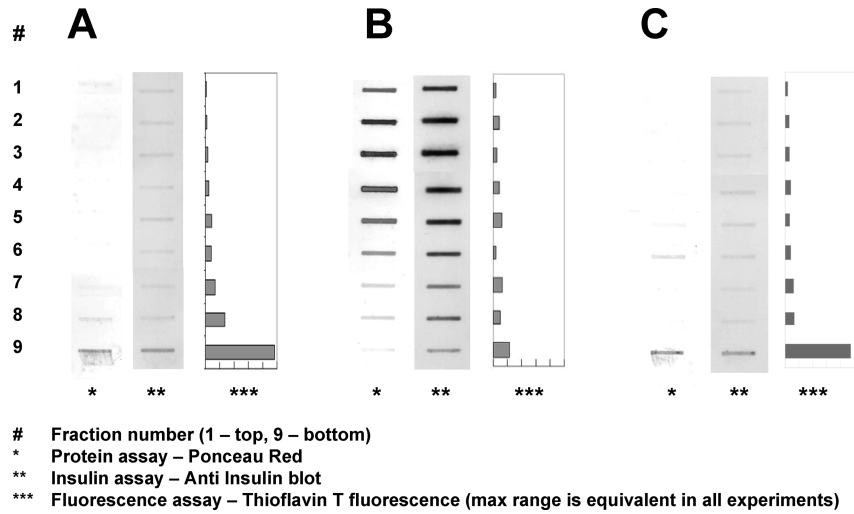

FIGURE 7: Density gradient fractionation of insulin fibrils and prefibrillar assemblies. (A) Insulin 50 μM after incubation for 48 h in DDW pH 2 at 50 °C. (B) Insulin that was incubated in the presence of 50 μM phenolsulfonphthalein. (C) Insulin that was incubated in the presence of 50 μM phenolphthalein.

insulin was present only in the lowest fraction (fraction 9) of the density gradient (Figure 7A). This fraction showed both high protein concentration and high Thioflavin T fluorescence suggesting that it was composed mostly of aggregated fibrillar insulin. Although the strongest interaction with anti-insulin antibody was also evident in this fraction, the relatively low band density maybe contributed to a low degree of interaction of the antibody with fibrillar insulin. A similar fractionation pattern was achieved when phenolphthalein was added to insulin during incubation suggesting no inhibitory effect whatsoever (Figure 7C). In contrast, phenolsulfonphthalein caused a significant difference in the fractionation pattern of insulin. When phenolsulfonphthalein was added to insulin, the latter was present in fractions 1−6 with a maximum insulin level in fractions 3 and 4, which represent low molecular weight prefibrillar assemblies, and none in the high molecular weight fraction, indicating that no fibril was formed (Figure 7B). In general, the fractionation pattern resulting from Ponceau red assay and anti-insulin blotting was very similar, meaning that the inhibitors did not interfere with insulin−antibody interactions. A minor exception was observed in the high molecular weight fraction in the bottom of the gradient with phenolsulfonphthalein, which shows some difference in the relative intensities of Ponceau red staining and the anti-insulin stain.

NMR Measurements. The 1D and TOCSY NMR spectra of samples of $hIAPP_{20-29}$ alone or with a 1:4 molar ratio to ligands were taken (Figure 8). This ratio gave sufficient deviations in chemical shifts of the complex, without losing sensitivity due to a large excess of one component of the complex. The amide resonances of residues 21−27 were assigned unambiguously according to their TOCSY patterns; residues Ser28 and Ser29 were not specifically assigned (Table 1).

The deviations in amide chemical shift are shown in Figure 9, where the strong deviation of Ile26 upon binding phenolsulfonphthalein is evident. This deviation is on the scale of 15 Hz and is more than five times the deviation of any other amide. The aromatic protons of Phe23 also showed slight chemical shift deviations upon binding phenolsulfonphthalein: The HD and HZ aromatic protons of Phe23 showed a downfield deviation of about less than 1.2 Hz, and the resolved upper-field shift of the HE triplet showed an upfield deviation of twice that value. The aromatic protons of Phe23 showed a downfield shift of 3.0 Hz upon binding phenolphthalein, but the shift is uniform for all the aromatic protons (Figure 10).

The samples of $hIAPP_{20-29}$ and each ligand were compared to samples of each ligand alone. The pH values were within 0.1 unit of each other and were all acquired at 25 °C. The chemical shifts of the ligands did not show any significant change upon binding (data not shown), presumably because the 4:1 excess masked any such change.

DISCUSSION

The search for small-molecule inhibitors for treating amyloidogenic diseases is an ongoing scientific challenge whose goal is to discover safe, specific and highly efficient compounds that will inhibit the formation of the most cytotoxic intermediates of amyloidogenic protein aggregates.

Polyphenols, a group of natural and synthetic small molecules, were independently shown to have an inhibitory effect on amyloid fibril formation. This phenomenon was mostly attributed to the antioxidative nature of these compounds. Nevertheless, several of these reports have suggested that structural properties of the polyphenol compounds may be considered as affecting their inhibitory nature.

We have previously suggested that phenolsulfonphthalein, a synthetic small molecular compound that has been used for many years in several medical diagnostic procedures, is an effective inhibitor of hIAPP fibril formation *in vitro*. This polyphenol also inhibited the toxic effect of hIAPP in cell culture models of type 2 diabetes. Furthermore, experimental and theoretical studies suggest that aromatic interactions play an important role in many cases of amyloid protein self-assembly by affecting the directionality and orientation needed for this process (*14, 21–30*). We have also suggested that polyphenols and their polyaromatic nature may affect amyloid fibril formation by specific aromatic interactions among their phenolic rings and aromatic residues in the amyloidogenic sequence, and that a specific structural conformation is necessary for interacting with the β-sheet and stabilizing the inhibitor−protein complex (*13*).

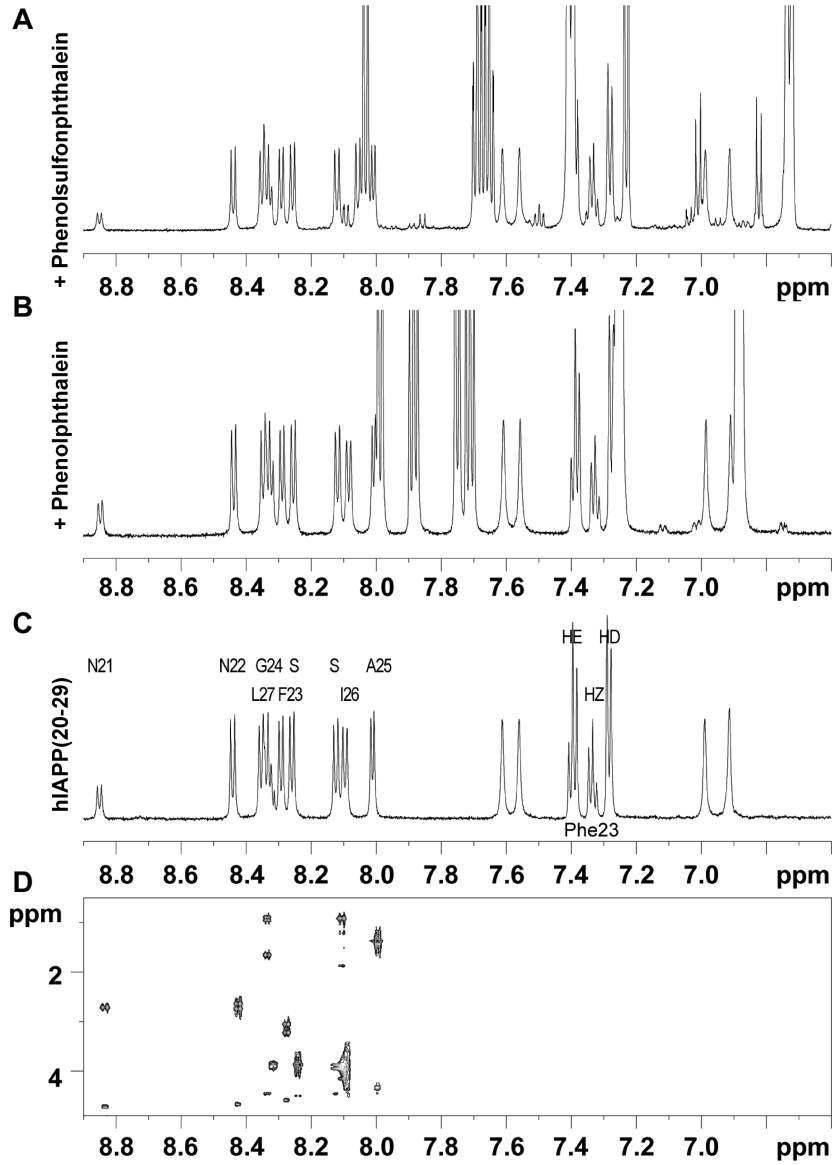

FIGURE 8: 1D NMR spectra of ligands and $hIAPP_{20-29}$. $hIAPP_{20-29}$ bound to (A) phenolsulfonphthalein and (B) phenolphthalein and the (C) 1D and (D) TOCSY spectra of unbound $hIAPP_{20-29}$.

Table 1: Amide Chemical Shifts of hIAPP(20−29) (ppm)

	N22	F23	G24	A25	I26	L27	S	S
hIAPP(20−29)	8.442	8.293	8.333	8.012	8.086	8.354	8.124	8.260

Here we provide further experimental evidence *in vitro* that phenolsulfonphthalein is a specific amyloid inhibitor. Using the core amyloidogenic peptides of hIAPP, NFGAILSS and SNNFGAILSS peptides, which serve as models for hIAPP aggregation, we show that phenolsulfonphthalein efficiently inhibited aggregation and fibril formation using a turbidity assay and electron microscopy (Figures 2–4). Furthermore, phenolsulfonphthalein inhibited full-length $hIAPP_{1-37}$ fibril formation using both a Thioflavin T fluorescence assay and electron microscopy (Figure 5). These results are in agreement with our previous findings that phenolsulfonphthalein inhibited $hIAPP_{1-37}$ fibril formation in a concentration-dependent manner (*14*).

In contrast, phenolphthalein, a similar triaromatic compound which differs from phenolsulfonphthalein only in the lack of the sulfone group, had no inhibitory effect whatsoever, neither on the amyloidogenic peptides $hIAPP_{22-29}$ (NFGAILSS, Figure 2A) and $hIAPP_{20-29}$ (SNNFGAILSS, Figures 2B and 4), nor on $hIAPP_{1-37}$ (Figure 5). This result implies two optional mechanistic explanations: (a) the importance of the sulfone group, which is predominant in the aromatic ring of the amyloid specific Congo Red dye; (b) the differences between these two molecules in their three-dimensional structures. The main difference between the structures is in the angle between the plane of the two phenol rings and the central carbon atom (Figure 1C).

To better understand the inhibitory effect of phenolsulfonphthalein on prefibrillar assemblies, we compared the inhibitory pattern of phenolsulfonphthalein on amyloidogenic insulin to that of phenolphthalein. First, using Thioflavin T fluorescence we showed that phenolsulfonphthalein inhibits insulin fibril formation in a concentration-dependent manner with an IC_{50} of 1.5 μM (Figure 6), which is comparable to the IC_{50} value of 1 μM of phenolsulfonphthalein which we have reported previously with hIAPP (*14*). Then, using a density gradient fractionation assay, we demonstrated that insulin, under specific experimental conditions, forms high molecular weight structures with high Thioflavin T fluores-

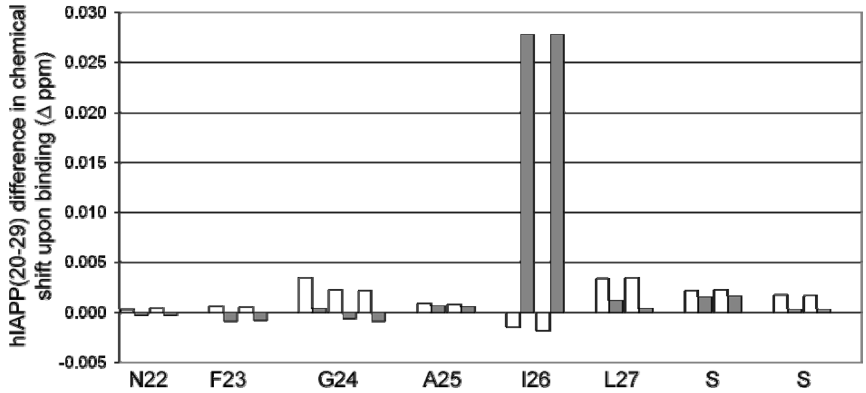

FIGURE 9: Chemical shift deviation of $hIAPP_{20-29}$ amide protons upon binding to phenolphthalein (white squares) and phenolsulfonphthalein (gray squares).

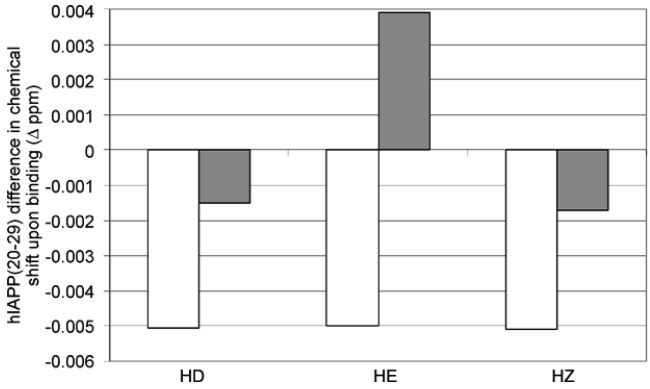

FIGURE 10: Chemical shift deviation of $hIAPP_{20-29}$ Phe23 aromatic protons upon binding to phenolphthalein (white squares) and phenolsulfonphthalein (gray squares).

cence that imply fibrillar structures (Figure 7A). As expected, adding phenolphthalein did not have any effect on the fractionation pattern, implying that phenolphthalein does not have an inhibitory effect on insulin fibril formation as well (Figure 7C). In contrast, adding phenolsulfonphthalein had a significant effect on insulin aggregation. No high molecular weight structures were formed, and most of the protein was in the first upper fractions, implying low molecular weight structures with low Thioflavin T fluorescence levels (Figure 7B). Taken together, these results imply that the interaction of phenolsulfonphthalein with hIAPP and insulin is highly specific and aimed toward the early stage of prefibrillar assembly formation. Density gradient separation provides an efficient tool for studying the mechanism of inhibition. The advantage of this fractionation method is that it combines both an analytical tool for molecular weight based analysis and a tool for separation for further characterization of the fractionated assemblies.

The NMR results show that the most significant chemical shift deviation upon binding phenolsulfonphthalein is that of the amide proton of Ile26. The deviations in the aromatic protons of Phe23 upon binding (Figure 10) are evident for all the peaks, but the deviation is the same for binding to phenolphthalein, whereas there is a difference in deviation for binding to phenolsulfonphthalein. These results are consistent with the molecular dynamic simulation results of Duan and co-workers (*31*), which showed that phenolsulfonphthalein interacts strongly with the side chains of Phe, Leu and Ile, with no interactions with main-chain hydrogens, and, although they note a slight increase in the rigidity of the phenolsulfonphthalein ligand itself upon binding, they found a similar distribution of torsion angles as in the free molecule. The most significant interactions we detected were between the phenolsulfonphthalein and the hydrophobic Ile amide proton, and we also found an effect on the Phe aromatic residue. Apart from this latter interaction, we saw no significant interactions with main-chain hydrogens of the peptide and, despite its 4:1 molar ratio, the ligand showed no deviations in chemical shift upon binding, indicating no strong change in its torsion angle.

The lactone ring of phenolphthalein and the sulfone ring of phenolsulfonphthalein can adopt both open and closed structures. All measurements were performed at physiological pH or lower: These are below the pK_a of all ligands, such that the major isomers of both ligands should be in their closed ring forms. The NMR spectra showed a dominant species in solution for phenolsulfonphthalein and phenolphthalein of 98.9% and 100%, respectively (Figure 8 A and B), indicating that this is the active isomer. Since no dependence between the inhibitory ability of the compounds and pH was noticed, we speculate that the ring structures do not tremendously influence protein−inhibitor interactions.

Structural comparison of the 3D structures of phenolsulfonphthalein (*32*) and phenolphthalein (*33*) (Figure 1C) may contribute to a better understanding of the interaction pattern between amyloidogenic proteins and small aromatic polyphenol compounds. Phenolsulfonphthalein was shown to bind hydrophobic side chains with its aromatic rings, leaving its hydrophilic SO_3 and OH free to form hydrogen bonds with the aqueous environment (*31*), which may be part of the mechanism by which the monomers or protofibrils are stabilized and prevented from further aggregation. These structural aspects are not yet resolved, and further analysis is necessary to determine the main factors affecting the interaction between the small molecule inhibitors and amyloidogenic proteins. We are currently analyzing structure-based data of various polyphenols to better approach this issue.

As earlier discussed, the development and production of novel drug candidates to treat amyloid-associated disease represent a true and acute medical need. We suggest that phenolsulfonphthalein may be an excellent lead for the development of an efficient, safe, and specific small molecule fibrillization inhibitor for amyloidogenic disease therapy. Further *in vivo* experiments with derivatives of phenolsulfonphthalein that improve its cellular penetration will enable better evaluation of this concept.

ACKNOWLEDGMENT

We thank Yaacov Delarea for his help in TEM microscopy. We also appreciate Osnat Zomer and Michal Shtilerman for their research project which is described in the last results section.

REFERENCES

1. Stefani, M., and Dobson, C. M. (2003) Protein aggregation and aggregate toxicity: new insights into protein folding, misfolding diseases and biological evolution. *J. Mol. Med. 81*, 678–699.
2. Ross, C. A., and Poirier, M. A. (2004) Protein aggregation and neurodegenerative disease. *Nat. Med.* 10 Suppl., S10−S17.
3. Jahn, T. R., and Radford, S. E. (2005) The Yin and Yang of protein folding. *FEBS J. 272*, 5962–5970.
4. Soto, C. (2003) Unfolding the role of protein misfolding in neurodegenerative diseases. *Nat. Rev. Neurosci. 4*, 49–60.
5. Makin, O. S., and Serpell, L. C. (2002) Examining the structure of the mature amyloid fibril. *Biochem. Soc. Trans. 30*, 521–525.
6. Hoppener, J. W., Ahren, B., and Lips, C. J. (2000) Islet amyloid and type 2 diabetes mellitus. *N. Engl. J. Med. 343*, 411–419.
7. Clark, A., and Nilsson, M. R. (2004) Islet amyloid: a complication of islet dysfunction or an aetiological factor in Type 2 diabetes? *Diabetologia 47*, 157–169.
8. Meier, J. J., Kayed, R., Lin, C. Y., Gurlo, T., Haataja, L., Jayasinghe, S., Langen, R., Glabe, C. G., and Butler, P. C. (2006) Inhibition of human IAPP fibril formation does not prevent beta-cell death: evidence for distinct actions of oligomers and fibrils of human IAPP. *Am. J. Physiol. Endocrinol. Metab. 291*, E1317-E1324.
9. Cohen, F. E., and Kelly, J. W. (2003) Therapeutic approaches to protein-misfolding diseases. *Nature 426*, 905–909.
10. Zhao, B. (2005) Natural antioxidants for neurodegenerative diseases. *Mol. Neurobiol. 31*, 283–294.
11. Yang, F., Lim, G. P., Begum, A. N., Ubeda, O. J., Simmons, M. R., Ambegaokar, S. S., Chen, P. P., Kayed, R., Glabe, C. G., Frautschy, S. A., and Cole, G. M. (2005) Curcumin inhibits formation of amyloid beta oligomers and fibrils, binds plaques, and reduces amyloid in vivo. *J. Biol. Chem. 280*, 5892–5901.
12. Lim, G. P., Chu, T., Yang, F. S., Beech, W., Frautschy, S. A., and Cole, G. M. (2001) The curry spice curcumin reduces oxidative damage and amyloid pathology in an Alzheimer transgenic mouse. *J. Neurosci. 21*, 8370–8377.
13. Porat, Y., Abramowits, A., and Gazit, E. (2006) Inhibition of amyloid fibril formation by polyphenols: Structural similarity and aromatic interactions as a common inhibition mechanism. *Chem. Biol. Drug. Des. 67*, 27–37.
14. Porat, Y., Mazor, Y., Efrat, S., and Gazit, E. (2004) Inhibition of islet amyloid polypeptide fibril formation: a potential role for heteroaromatic interactions. *Biochemistry 43*, 14454–14462.
15. Dunea, G., and Freedman, P. (1968) Renal Clearance Studies. *J. Am. Med. Assoc. 205*, 170–171.
16. Hobsley, M., and Silen, W. (1969) Use of an Inert Marker (Phenol Red) to Improve Accuracy in Gastric Secretion Studies. *Gut 10*, 787–788.
17. Speck, G. (1970) 22 Years Experience with Phenosulfonphthalein (Speck) Test for Determination of Tubal Patency. *Fertil. Steril. 21*, 28–29.
18. Ward, R. V., Jennings, K. H., Jepras, R., Neville, W., Owen, D. E., Hawkins, J., Christie, G., Davis, J. B., George, A., Karran, E. H., and Howlett, D. R. (2000) Fractionation and characterization of oligomeric, protofibrillar and fibrillar forms of beta-amyloid peptide. *Biochem. J. 348*, 137–144.
19. Bax, A., and Davis, D. G. (1985) MLEV-17 based two-dimensional homonuclear magnetization transfer spectroscopy. *J. Magn. Reson. 65*, 355–360.
20. Gazit, E. (2005) Mechanisms of amyloid fibril self-assembly and inhibition. Model short peptides as a key research tool. *FEBS J. 272*, 5971–5978.
21. Gazit, E. (2002) A possible role for p-stacking in self-assembly of amyloid fibrils. *FASEB J. 16*, 77–83.
22. Makin, O. S., Atkins, E., Sikorski, P., Johansson, J., and Serpell, L. C. (2005) Molecular basis for amyloid fibril formation and stability. *Proc. Natl. Acad. Sci. U.S.A. 102*, 315–320.
23. Jack, E., Newsome, M., Stockley, P. G., Radford, S. E., and Middleton, D. A. (2006) The organization of aromatic side groups in an amyloid fibril probed by solid-state 2H and 19F NMR spectroscopy. *J. Am. Chem. Soc. 128*, 8098–8099.
24. Jones, S., Manning, J., Kad, N. M., and Radford, S. E. (2003) Amyloid-forming peptides from beta(2)-microglobulin-Insights into the mechanism of fibril formation in vitro. *J. Mol. Biol. 325*, 249–257.
25. Naito, A., Kamihira, M., Inoue, R., and Saito, H. (2004) Structural diversity of amyloid fibril formed in human calcitonin as revealed by site-directed C-13 solid-state NMR spectroscopy. *Magn. Reson. Chem. 42*, 247–257.
26. Tartaglia, G. G., Cavalli, A., Pellarin, R., and Caflisch, A. (2004) The role of aromaticity, exposed surface, and dipole moment in determining protein aggregation rates. *Protein Sci. 13* 1939–1941.
27. Zanuy, D., Porat, Y., Gazit, E., and Nussinov, R. (2004) Peptide sequence and amyloid formation: Molecular simulations and experimental study of a human islet amyloid polypeptide fragment and its analogs. *Structure 12*, 439–455.
28. Wu, C., Lei, H. X., and Duan, Y. (2005) The role of Phe in the formation of well-ordered oligomers of amyloidogenic hexapeptide (NFGAIL) observed in molecular dynamics simulations with explicit solvent. *Biophys. J. 88*, 2897–2906.
29. Colombo, G., Daidone, I., Gazit, E., Amadei, A., and Di Nola, A. (2005) Molecular dynamics simulation of the aggregation of the core-recognition motif of the islet amylolid polypeptide in explicit water. *Proteins 59*, 519–527.
30. De Felice, F. G., Vieira, M. N. N., Saraiva, L. M., Figueroa-Villar, J. D., Garcia-Abreu, J., Liu, R., Chang, L., Klein, W. L., and Ferreira, S. T. (2004) Targeting the neurotoxic species in Alzheimer's disease: inhibitors of A beta oligomerization. *FASEB J. 18*, 1366–1372.
31. Wu, C., Lei, H., Wang, Z., Zhang, W., and Duan, Y. (2006) Phenol red Interacts with the protofibril-like oligomers of an amyloidogenic hexapeptide NFGAIL through both hydrophobic and aromatic contacts. *Biophys. J. 91*, 3664–3672.
32. Yamaguchi, K., Tamura, Z., and Maeda, M. (1997) Molecular structure of the zwitterionic form of phenolsulfonphthalein. *Anal. Sci. 13*, 521–522.
33. Fitzgerald, L. J., and Gerkin, R. E. (1998) Phenolphthalein and 3′,3″-Dinitrophenolphthalein. *Acta Crystallogr. C 54*, 535–539.
34. NIIRD. (1990) Drugs in Japan (Ethical Drugs) pp 930, Yakugyo. Jiho Co., Ltd., Tokyo.
35. Mason, M. M., Cate, C. C., and Baker, J. (1971) Toxicology and Carcinogenesis of Various Chemicals Used in the Preparation of Vaccines. *Clin. Toxicol. 4*, 185–204.

BI800043D